TITLE

Dissecting sources of variability in patient response to targeted therapy: anti-HER2 therapies as a case study

RUNNING TITLE

Dissecting sources of variability in response to targeted therapy

AUTHORS

Timothy Qi, B.S.,[1] and Yanguang Cao, Ph.D.[1,2*]

AFFILIATIONS

[1]Division of Pharmacotherapy and Experimental Therapeutics, Eshelman School of Pharmacy, The University of North Carolina at Chapel Hill, Chapel Hill, NC 27599, USA

[2]Lineberger Comprehensive Cancer Center, The University of North Carolina at Chapel Hill, Chapel Hill, NC 27599, USA

DATA AVAILABILITY STATEMENT

The data that support the findings of this study will be made available from the corresponding author upon reasonable request.

WORD COUNT (excluding Methods): 2926

***Lead Contact.** Email: yanguang@unc.edu. Address: 301 Pharmacy Ln, Chapel Hill, NC 27599

DECLARATIONS OF INTEREST

T.Q. is a contractor for Hatteras Venture Partners.

KEYWORDS

HER2, tyrosine kinase inhibitor, breast cancer, free drug hypothesis, population pharmacokinetics, tumor evolution, tumor growth modeling, growth rate metrics

ABBREVIATIONS

AUC, area under the curve
BID, twice daily
BOR, best overall response
CDK, cyclin-dependent kinase
DNTP, death or non-target progression
FDA, Food & Drug Administration
FISH, fluorescence in situ hybridization
GEC_{50}, concentration at half-maximal growth rate inhibition effect
GR, growth rate inhibition [metrics]
GR_{inf}, growth rate inhibition at infinite drug concentration
HER, human epidermal growth factor receptor
HMS LINCS, Harvard Medical School Library of Network-based Cell Signatures
IHC, immunohistochemistry
ORR, objective response rate
PD, pharmacodynamics
PFS, progression-free survival
PI3Kα, phosphoinositide 3-kinase alpha
PK, pharmacokinetics
PPB, plasma protein bound
QD, once daily
TKI, tyrosine kinase inhibitor

ABSTRACT

Background and Purpose: Despite their use to treat cancers with specific genetic aberrations, targeted therapies elicit heterogeneous responses. Sources of variability are critical to targeted therapy drug development, yet there exists no method to discern their relative contribution to response heterogeneity.

Experimental Approach: We use HER2-amplified breast cancer and two agents, neratinib and lapatinib, to develop a platform for dissecting sources of variability in patient response. The platform comprises four components: pharmacokinetics, tumor burden and growth kinetics, clonal composition, and sensitivity to treatment. Pharmacokinetics are simulated using population models to capture variable systemic exposure. Tumor burden and growth kinetics are derived from clinical data comprising over 800,000 women. The fraction of sensitive and resistant tumor cells is informed by HER2 immunohistochemistry. Growth rate-corrected drug potency is used to predict response. We integrate these factors and simulate clinical outcomes for virtual patients. The relative contribution of these factors to response heterogeneity are compared.

Key Results: The platform was verified with clinical data, including response rate and progression-free survival (PFS). For both neratinib and lapatinib, the growth rate of resistant clones influenced PFS to a higher degree than systemic drug exposure. Variability in exposure at labeled doses did not significantly influence response. Drug potency strongly influenced responses to neratinib. Variability in patient HER2 immunohistochemistry scores influenced responses to lapatinib. Exploratory twice daily dosing improved PFS for neratinib but not lapatinib.

Conclusion and Implications: The platform can dissect sources of variability in response to target therapy, which may facilitate decision-making during drug development.

INTRODUCTION

Patient response to targeted therapy is highly variable and difficult to predict. Multiple factors contribute to diverse patient responses to targeted therapy, including but not limited to drug pharmacokinetics (PK) and biodistribution [1], tumor growth characteristics [2], clonal composition [3], and tumor sensitivity or resistance [4]. Understanding the source of response variability can be valuable for decisions made during drug development concerning dose selection, patient stratification, and therapeutic benefit evaluation. However, some of these factors are challenging to characterize during clinical studies. For example, it is implausible to measure tumor growth rates without treatment in a metastatic disease setting. As a result, the relative contribution of these factors to discrepancies in drug efficacy within diverse patient populations remains largely undefined. Simulations informed by high volumes of historical clinical data and drug potency parameters measured during early-stage drug discovery may be convenient and intuitive tools for dissecting sources of variability in patient response and informing decision-making during drug development.

Here, we use HER2-amplified metastatic breast cancer as a model system to decompose sources of variability in response to HER2 tyrosine kinase inhibitors (TKI). Given the routine clinical assessment of HER2 amplification in patients with newly diagnosed metastatic breast cancer, we assessed whether a pharmacokinetics/pharmacodynamics/tumor growth (PK/PD/TG)-based model could be applied to predict the efficacy of HER2 TKIs in patients with different levels of HER2 amplification. Such a model might also be useful in determining whether variability in response to approved HER2 TKIs depend on tumor-intrinsic features, like growth rate and HER2+ fraction, or drug-specific properties, like PK and biodistribution.

Toward this end, we have developed a PK/PD/TG model for decomposing sources of variability between responders and non-responders. We simulate the highly variable PK of two HER2 TKIs, neratinib and lapatinib, and their therapeutic effects on tumor growth and progression. We also model a wide range of tumor sensitivity to therapy as informed by drug potency in cell lines with varying HER2 expression and population-level diversity in HER2 immunohistochemistry (IHC) scores. These data are integrated into a virtual patient population to dissect the sources of variability in patient response.

There are two key aspects of our approach. One is the use of population PK models to simulate drug PK and variability in patients. Population PK models and parameter estimates for investigational and approved drugs are usually readily available to sponsors. Using the drug sponsors' population PK models ensures our simulations recapitulate a wide range of possible drug exposures. This is of critical importance, as drug exposure can vary dramatically between patients. Second, we explored the therapeutic effect in a tumor comprising mixed subpopulations of sensitive (HER2-amplified) and resistant (HER2-negative) cells. The clonal composition of these cells in a given tumor was informed by patient HER2 IHC scores. We considered subpopulation-specific cytostatic and cytotoxic effects using the growth rate inhibition metrics developed by Hafner et al. [4]. These metrics correct for differences in growth rates among cell lines, which can otherwise confound interpretations of drug potency. Recent publications showcase the added value of using growth rate metrics for predicting in vivo responses from in vitro data alone [5] and support the further elaboration of this approach for drug development.

METHODS

Modeling framework overview

The framework is shown in Fig. 1A. First, we used population PK models to derive drug exposure in patients. Next, we constructed a virtual HER2-positive patient population from large clinical datasets of HER2 IHC and tumor growth kinetics. We then used the in vitro GR metrics to determine sensitivity and resistance of tumor cellular subpopulations to treatment. Finally, we integrated these sources of variability to model the response of tumors with mixed populations to HER2 TKI treatment.

Variability in systemic drug exposure

For neratinib, a population PK model was used to simulate plasma concentration vs. time profiles [6]. Among all significant covariates, we included the effects of normally distributed age on k_a and central volume, as well as the effects of lognormally distributed weight on clearance and central volume. No transporter-mediated uptake into cells was reported. We also assumed that patients would take the drug with a standard, low-fat breakfast under real-world conditions.

For lapatinib, a structurally similar population PK model was used, the only difference being that drug absorption was modeled as a T_{lag}-delayed zero-order input followed by a first-order input at the rate k_a [7]. We included the effects of normally distributed age on k_a and excluded the effects of ethnicity and race on other parameters. No transporter-mediated uptake into cells was reported. We also assumed that patients would take the drug with a standard, low-fat breakfast under real-world conditions.

Free drug concentrations were simulated to inform tumor concentrations based on the Free Drug Hypothesis [8]. Prior to PK/PD simulation, we used the following equation to estimate the average unbound steady-state concentrations of alpelisib (PI3Kα), abemaciclib (CDK4/6), palbociclib (CDK4/6), ribociclib (CDK4/6), lapatinib (HER1/2), and neratinib (HER1/2/4):

$$C_{ss,free} = \frac{X/\tau}{CL/F} \cdot (1 - PPB)$$

Where X is the approved dose, τ is the approved dosing interval, and CL/F is the apparent clearance upon oral administration. PPB is the protein-bound fraction reported in publicly available US Food & Drug Administration (FDA) multidisciplinary review documents for each drug; the exception was neratinib, where the PPB in plasma samples from healthy volunteers was reported to be significantly lower than the in vitro PPB. For lapatinib, the reported PPB of "> 99%" was estimated as 99.5%. The following values were used for each drug: abemaciclib (X = 200 mg, τ = 12 hours, CL/F = 38 L/hour, PPB = 96.3%), alpelisib (X = 300 mg, τ = 24 hours, CL/F = 9 L/hour, PPB = 89.2%), lapatinib (X = 1250 mg, τ = 24 hours, CL/F = 114 L/hour, PPB = 99.5%), neratinib (X = 240 mg, τ = 24 hours, CL/F = 195 L/hour, in vitro PPB = 99%, in vivo PPB = 88%), palbociclib (X = 125 mg, τ = 24 hours, CL/F = 81 L/hour, PPB = 85%), and ribociclib (X = 600 mg, τ = 24 hours, CL/F = 26 L/hour, PPB = 70%). As it is generally thought that only free drug is available to interact with pharmacologically relevant targets in vivo [8], [9],

GEC_{50} values of cell lines were corrected for PPB to estimate sensitivity to free drug concentrations.

Variability in tumor size and composition

To estimate the baseline tumor burden at diagnosis of metastatic disease, we used data from a study of 819,647 women in the Surveillance, Epidemiology and End Results (SEER) registry [10]. To calculate the distribution of baseline tumor burden among patients diagnosed with metastatic disease, we multiplied the baseline tumor burden of all patients at diagnosis by the probability of a patient to have metastatic disease given a particular tumor burden (Fig. 1B). For tumor size probabilities reported over size intervals, we assumed a uniform distribution over the interval and calculated probabilities in diameter increments of 1 mm. A lognormal fit to these data yielded a mean log tumor diameter (mm) of 3.624 and a standard deviation of 0.668. Baseline diameters were converted to volumes for simulation, assuming approximately spherical tumors (Fig. 1C). Parameters used for generating virtual populations and treatment simulations are provided in Table S1.

As HER2 TKIs are indicated for HER2+ breast cancer patients, we needed to estimate the cellular fraction of each tumor that was HER2 amplified. HER2 positivity is currently defined as IHC scores of IHC3+ or IHC2+ with amplification on orthogonal fluorescence in situ hybridization (FISH) assay. The proportion of IHC3+ and IHC+ patients among all HER2+ patients was calculated from 1,522 samples reported in a 12-year, single-center study [11] (Fig. 1D). For simplicity, we assumed each tumor harbored one sensitive (HER2-amplified) and one resistant (HER2-negative) population of cells with different levels of sensitivity to HER2 TKIs.

Variability in tumor sensitivity and resistance

Once a virtual patient was designated as IHC3+ or IHC2+, a fraction f_{sens} of their tumor cells was designated as sensitive, while $f_{res} = 1 - f_{sens}$ was designated as resistant. By definition, 10 – 30% of cancer cells in IHC2+ tumors are HER2 amplified, compared to 30 – 100% of cells within IHC3+ tumors. Within these two strata, we assumed HER2 amplification was uniformly distributed.

To calibrate the effect of drug concentrations on tumor growth, the in vitro growth rate (GR) metrics of 75 human breast cancer cell lines under treatment with alpelisib, abemaciclib, palbociclib, ribociclib, lapatinib, and neratinib were identified from the literature [4], [12]. Data are presented in Fig. 2A. For use in the model, the HER2 status and clinical subtype of each cell line was cross-referenced with data from [13]. Cell lines with unknown or inconsistent HER2+ status across publications were excluded. Drug potency (GEC_{50}), efficacy (GR_{inf}), and Hill coefficient parameters of HER2+ cell lines were sampled to generate HER2 TKI-sensitive cell populations, while the parameters for Basal A and Basal B cell lines were sampled to generate resistant populations. GEC_{50} values were adjusted for PPB as described above. The GR metrics for neratinib and lapatinib are presented in Fig. 2B and Fig. S1, respectively.

Modeling responses to HER2 TKI

Tumor growth with and without treatment was modeled using a generalized logistic model with an exponent of 0.25 [14] (Fig. 1C), which has been validated to faithfully characterize the growth kinetics of breast tumors in a study of 395,188 women [2]. The *b*

growth parameter estimated in this study was lognormally distributed with a mean of 1.38 and variance of 1.36 for women under the age of 60. This corresponds to a geometric mean k_g = 1.66 x 10^{-4} hours, or 2.78 x 10^{-2} weeks. The equations used to model changes in the abundance (volume) of sensitive and resistant cell populations over time were:

$$\frac{dSens}{dt} = k_{g,sens} N_{sens} \left(1 - \frac{N_{sens} + N_{res}}{K}\right)^4 log_2(1 + Effect_{sens})$$

$$\frac{dRes}{dt} = k_{g,res} N_{res} \left(1 - \frac{N_{sens} + N_{res}}{K}\right)^4 log_2(1 + Effect_{res})$$

$$\frac{dTumor}{dt} = \frac{dRes}{dt} + \frac{dSens}{dt}$$

Where N represents the volume of the population and K represents the carrying capacity (diameter = 128 mm [2]). The effects of drug on tumor growth, $Effect_{sens}$ and $Effect_{res}$, were calculated as follows [4]:

$$Effect = GR_{inf} + \frac{1 - GR_{inf}}{1 + \left(\frac{Free\ drug}{GEC_{50}}\right)^h}$$

Where *h* is a Hill coefficient estimated for a given cell line's relationship between drug concentrations, GR_{inf}, and GEC_{50}. Of note, a proportion (27%) of neratinib's therapeutic effect is attributed to active metabolites [6]. We therefore multiplied free neratinib concentrations by 1 / (1 – 0.27) when calculating $Effect_{sens}$ and $Effect_{res}$ to adjust for expected metabolite activity.

Analysis and software

Virtual populations were generated in MATLAB R2020b. Treatment simulations were performed in Simulx 2020. Statistical analyses were performed in MATLAB R2020b. Diameters were "measured" by sampling from simulations every 6 or 8 weeks to assess for progression-free survival (PFS), mirroring the frequency of radiographic assessment in clinical trials. PFS was evaluated per RECIST v1.1 criteria, which designate target lesion diameter increases of ≥ 20% from nadir and at least 5 mm in absolute terms as progressive disease [15]. Importantly, events such as the appearance of new metastases, enlargement of non-target lesions, and death from any cause are also classified as progressive disease. We termed these events "DNTP", or Death or Non-target Progression, and modeled the daily probability of patients to progress due to DNTP at the empirically estimated rate of 1.5 x 10^{-4} events/mm of tumor diameter/day.

Objective response rates (ORR) were also evaluated per RECIST v1.1. This required the calculation of best overall response (BOR) for each patient. To do so, diameter measurements sampled from simulations every 6 or 8 weeks were compared to baseline tumor diameters. The smallest non-baseline tumor measurement was used to evaluate BOR. Patients with BOR diameter reductions of at least 30% from baseline were considered responders. ORR was calculated by dividing the fraction of responders by the total number of patients.

RESULTS

Tumor sensitivity and resistance to targeted therapies is heterogeneous

We initially questioned whether the steady-state unbound concentrations of several targeted therapies at their approved doses for the treatment of metastatic breast cancer were above or below their in vitro potency, as measured by PPB-adjusted GEC_{50}. Plotting the PPB-adjusted GEC_{50} of breast cancer cell lines [4], [12] against the estimated $C_{ss,free}$ (Fig. 2A, see Methods) of 6 different drugs revealed significant differences in predicted response. The majority of cell lines in the dataset possessed GEC_{50} below the $C_{ss,free}$ of abemaciclib, neratinib, and palbociclib, but not alpelisib, lapatinib, and ribociclib (Fig. 1). While these cell lines may not fully reflect the mixed cellular populations in patients, it is reassuring that HER2-amplified cell types in particular tended to have sensitivities below the predicted $C_{ss,free}$ of HER2 TKIs neratinib and lapatinib. No such enrichment of HER2-amplified cell lines was noted for the PARP inhibitors abemaciclib, palbociclib, and ribociclib, nor for the PI3Kα inhibitor alpelisib. These data support the fidelity of GR metrics for characterizing and discriminating sensitivity and resistance to HER2 TKIs across diverse cell lines.

Plasma free neratinib is closely associated with patient response and confers therapeutic effect beyond target lesions

We created a virtual HER2+ breast cancer population and simulated patient response to neratinib (see Methods). The population PK of neratinib was simulated using a two-compartment model with sequential first-order absorption, T_{lag}, and first-order elimination (Fig. 3A-B) [6], [16], [17]. A generalized logistic growth model was used to describe the growth of a two-population tumor with different subpopulation sensitivities to neratinib (Fig. 3C-D) [2], [14].

We explored several possibilities for tumor suppressive effects, including total- and free-drug concentration-driven tumor growth inhibition of target lesions as well as indirect (unobserved) suppression of the growth of non-target and new lesions. When only target lesions were considered, tumor growth inhibition driven by total drug concentrations resulted in an overestimation of PFS and ORR (Fig. S2) [16]. This was not entirely unexpected, as progression from target lesions only reflects a subset of patients; many breast cancer progression events are due to death, new metastases, or non-target lesion progression while patients are still under therapy [18]. The use of free neratinib concentrations improved concordance and matched the target lesion response rates reported in [16] (31.6% simulated vs. 30.3% reported), but still overestimated PFS (Fig. 3E-F).

We found the indirect tumor suppressive effect on non-target and new lesions to be critical for producing clinically consistent outcomes. For tumors that were already large at baseline, modeling drug effect on target lesions alone may overpredict patient response as these patients are at a higher risk of non-target progression and new lesions. Considering (1) the positive correlation between tumor burden and mortality and/or metastasis [10], and (2) more patients with metastatic breast cancer progress from non-target sources than target sources [18], we derived an additional time-variant probability of Death or Non-target progression (DNTP) for each patient that increased as a function of tumor burden. DNTP represents the instantaneous daily probability of a patient to die, experience new metastasis,

or exhibit non-target lesion growth and was estimated as 1.5×10^{-4} events/mm tumor diameter/day.

With free drug-driven tumor growth inhibition and indirect tumor burden-driven DNTP, the platform generated PFS estimates that matched well with clinical outcomes [16] (Fig. 3G). Interestingly, the risk of progression from non-target, DNTP sources was relatively consistent throughout the course of treatment, whereas the risk of progression from target lesions was highest toward the end of treatment (Fig. 3H). Free drug-driven PD with concomitant DNTP was carried forward for all additional simulations.

Patient response to neratinib is mostly influenced by tumor characteristics and less by systemic drug exposure

Having established the model's ability to reasonably recapitulate the clinical outcomes of neratinib, we proceeded to simulate 52 weeks of neratinib monotherapy in 1,000 virtual patients in search of tumor characteristics associated with longer PFS. Treatment with 240 mg QD neratinib prolonged median PFS from 15.5 to 18.3 weeks (Fig. 4A) and extended DNTP-free survival in 25.7% of patients (Fig. 4B).

Patients were stratified by tumor characteristics and systemic drug exposure (Fig. 4C). As expected, a greater baseline tumor burden correlated with shorter PFS. The growth rate of resistant cells and drug potency on sensitive cell populations were also great sources of variability in PFS (Fig. 4D). Patients with more sensitive cell populations or slower growth of resistant populations tended to have longer survival. In contrast, the growth of sensitive cell populations, drug potency on resistant cell populations, and drug PK parameters like clearance, area under the curve (AUC), and $C_{ss,trough}$ at the labeled dose did not significantly influence patient response and PFS (Fig. 4C). Interestingly, differences in HER2+ fraction were also insignificant to patient response.

Patients who achieved above-median PFS tended to have greater killing of sensitive cells and better control of resistant cell outgrowth than patients who did not (Fig. 4E). On an individual level, however, a diverse range of response dynamics was observed (Fig. 4F). Sensitive subpopulations could be completely eradicated in some patients, fully controlled in others, and completely insensitive in still others (Fig. 4F), raising the possibility of post-treatment changes to HER2+ fraction [19]. Collectively, these data suggest that tumor-intrinsic characteristics and cellular heterogeneity strongly influence patient responses to targeted therapy, and to a higher degree than inter-individual variability in drug PK at the approved doses.

Patient response to lapatinib is also largely explained by variability in tumor characteristics and cellular composition

To investigate the broader applicability of our modeling approach, we adjusted the PK/PD/TG model for another HER2 TKI, lapatinib (Fig. 5A). Simulations using the virtual breast cancer population, publicly available GR metrics [4], [12], and the original sponsor-developed population PK models reproduced the clinically observed PK, PFS, and ORR of 1500 mg QD lapatinib (Fig. 5B, Fig. S3) [7], [20]–[22]. As with neratinib, free plasma lapatinib was assumed to drive tumor suppressive effect while accounting for indirect effects on additional probability of progressive disease from DNTP.

Lapatinib monotherapy was predicted to improve median PFS to 17.4 weeks, from 15.1 weeks if untreated (Fig 5C). DNTP-free survival was also extended in 11.4% of patients (Fig. 5D). Similar to neratinib, tumor-intrinsic properties such as tumor burden and resistant cell growth rate differed between patients with longer and shorter PFS, while PK parameters did not (Fig. 5E). HER2+ fraction also impacted lapatinib outcomes, with the lowest quartile exhibiting markedly shorter PFS (Fig. 5F), while drug sensitivity did not. In contrast to neratinib, there was no difference in the killing of sensitive cells between patients who achieved above- and below-median PFS, although there was a difference in the control of resistant cell outgrowth (Fig. 5G).

Dose intensification may improve clinical response for neratinib but may not for lapatinib

Although there was only a modest relationship between PK variability and PFS under the approved doses of neratinib and lapatinib, we wondered whether BID dosing might improve tumor control and patient outcomes. To our surprise, doubling the dosing frequency improved outcomes for neratinib significantly more than for lapatinib, with 27% versus 2% deriving longer PFS from BID dosing (Fig. 6A-B). This suggests different levels of susceptibility of neratinib and lapatinib, at their approved doses, to significant changes in PK; 240 mg QD neratinib is perhaps in a steeper portion of its dose-response curve than 1500 mg QD lapatinib. Dose fractionation of neratinib into 120 mg BID to mitigate dose-limiting diarrhea did not significantly influence efficacy (Fig. S4) [6].

DISCUSSION

In this study, we integrated PK, tumor stage and growth characteristics, clonal composition, and tumor sensitivity and resistance to treatment into a PK/PD/TG modeling platform and simulated the antitumor efficacy of two HER2 TKIs in a virtual metastatic breast cancer population. Previous studies conducted to evaluate the interplay between PK and tumor characteristics and their influence on patient response have found both to be major sources of variability in patient response [1]. While we also found tumor growth parameters such as resistant cell growth rate to significantly contribute to PFS, we did not find a strong influence of drug PK on patient response to the assessed target therapies.

The finding that HER2+ positivity influenced clinical outcomes under lapatinib treatment is consistent with clinical observations [23]. It is not clear why a similar magnitude of effect was not observed in patients treated with neratinib. We also found the growth rate of resistance clones, analogous to tumor regrowth rate after progression, to be significant to patient response. Interestingly, growth rate after progression has been directly correlated with patient survival in non-small cell lung cancer and glioblastoma [24], [25]. A similar analysis has been conducted for HER2-negative breast cancer response to chemotherapy [26], though to our knowledge, no such work exists for HER2-positive breast cancer. Our results in the context of accumulating literature highlighting the importance of HER2+ fraction suggests a similar relationship may between regrowth rate and long-term outcomes may exist.

To recapitulate clinically observed PFS curves that account for progression from both target and non-target sources, a tumor burden-based risk of DNTP seems to be critical [10], [18]. Patients with metastatic disease may have discordant responses to therapy across metastases, confounding PFS based on changes in the target lesions [27], [28]. To our knowledge, DNTP rates have not been well characterized previously. As shown in our study, DNTP rate could be informed by the progression difference between target lesions and all lesions that are clinically observed per RECIST 1.1.

Two points should be kept in mind when interpreting this study. First, nonspecific protein binding is much higher in tumors than in blood for most small molecule therapeutics. For lapatinib specifically, Spector et al. [29] showed that total drug concentrations in xenograft tumors are slower clearing and at least 6-fold higher than in plasma. With substantial total drug accumulation in the tumor due to nonspecific binding, one would expect total drug-driven effect to result in even longer PFS than we have simulated here, therefore requiring a higher rate of DNTP to “bring down” the PFS curve. One major assumption of this work is that nonspecific proteins available for drug binding are always in great excess, leading to a constant f_{up} over time [30], [31]. Hypoalbuminemia does occur in breast cancer, although whether this meaningfully affects free drug concentrations is not known [32].

Second, the Free Drug Hypothesis is generally taken *prima facie* when translating drug PD from in vitro systems into living organisms [5], [8]. This draws from the assumption that drug nonspecifically bound to circulating plasma protein or extracellular parenchymal protein is unable to interact with its intended target – in this case, the intracellular kinase domain of HER2. Violations of the free drug hypothesis are generally driven by mechanisms that disturb steady state equilibria assumptions, such as drug transport proteins like P-glycoprotein (Pgp) or high tissue clearance rates relative to diffusion [8]. While lapatinib is a substrate for Pgp and breast cancer resistance protein (BCRP) [33], the direction of its transport is extracellular, such

that intracellular lapatinib concentrations are unlikely to be higher than what one would expect from free plasma concentrations. With no evidence to suggest transporter-mediated uptake into cancer cells, nor increased clearance from the tumor, we consider free drug concentrations to be an appropriate driver of PD for lapatinib [6], [9], [29]. Hypothetically, covalent inhibitors such as neratinib might cause receptor internalization, leading to longer PD than would be expected from free concentrations [34]. If de novo HER2 re-synthesis kinetics are faster than neratinib's half-life, however, we would expect this prolonged PD to be negligible [35].

Oncology drug developers may benefit from seriously considering free drug concentrations when predicting clinical efficacy from pre- and non-clinical data. With our emphasis on free drug concentrations, it might be tempting to use this study to support optimizing protein binding as a goal during early development. However, this would be misguided, as decreasing protein binding does not increase free drug AUC without a concomitant decrease in intrinsic clearance [36]. For drugs such as lapatinib, correcting for protein binding and comparing to GR metrics like GEC_{50} may have alerted investigators to the relatively minimal effect lapatinib would exert as a monotherapy [21]; indeed, lapatinib is only approved for use in combination with capecitabine. Previous studies that estimated brain tumor lapatinib concentrations did not consider nonspecific protein binding and used an oversimplified representation of the drug's pharmacokinetic variability [37]. Interestingly, the 0.61 tumor-to-blood ratio that was used is lower than the tumor accumulation ratio reported by Spector et al., though this may be due to differences in brain and peripheral drug distribution [29]. In any case, it may be useful to re-evaluate these studies in the context of blood brain barrier-mediated transport of free drug.

Developing a well-calibrated model with realistic characterization of inter-patient PK and tumor growth variability allowed us to explore alternative dosing regimens in a semi-realistic population. We were surprised to find substantial differences in the extent of benefit achieved with BID neratinib and lapatinib. Hypothetically, this suggests dose titration of lapatinib up to 1500 mg BID would be futile in most cases, whereas 240 mg BID neratinib would be reasonably likely to extend PFS. In practice, dose-limiting diarrhea may prevent the administration of more than 240 mg QD neratinib, highlighting that safety and tolerability can impose upper limits to the range of the free drug ER that can be explored [6]. Splitting the 240 mg dose into two 120 mg doses did not compromise efficacy of neratinib (Fig. S4), but did lower $C_{ss,max}$ without changing $C_{ss,avg}$. This may be an alternative to the currently on-label dose adjustment strategy, which recommends sequential dose reductions in increments of 40 mg.

HER2 was an unusually apt target on which to demonstrate modeling proof of concept, as HER2 amplification is routinely quantified in the clinic. In addition, widespread breast cancer screening efforts have generated volumes of data against which it is possible to calibrate models of tumor growth [2]. Based on these results, it may be useful to consider HER2+ fraction as a predictor of outcomes on HER2 targeted therapy; this may provide greater granularity than HER2 IHC scores. An immediate expansion of this approach would be to predict the efficacy of EGFR TKIs, as several groups have found EGFR mutation fraction to influence outcomes during treatment with EGFR mutation-selective therapies [38], [39]. Overall, our GR metric-based population PK/PD/TG modeling approach has potentially broad utility for decision-making during early drug development.

AUTHOR CONTRIBUTIONS

Conceptualization, T.Q. and Y.C.; Methodology, T.Q.; Software, T.Q.; Validation, T.Q.; Formal Analysis, T.Q.; Investigation, T.Q.; Resources, Y.C.; Data Curation, T.Q.; Writing – Original Draft, T.Q.; Writing – Review & Editing – T.Q. and Y.C.; Visualization – T.Q.; Supervision – Y.C.; Project Administration – T.Q. and Y.C.; Funding Acquisition – Y.C.

ACKNOWLEDGEMENTS

Figures were prepared in BioRender.

FUNDING

This work was supported by the National Institute of General Medical Sciences R35GM119661.

SUPPLEMENTAL MATERIALS

Table S1. Model parameters
Table S2. Patient characteristics of neratinib monotherapy trials
Table S3. Patient characteristics of lapatinib monotherapy trials
Figure S1. Lapatinib drug sensitivity
Figure S2. Neratinib pharmacodynamics using total or free drug
Figure S3. Lapatinib efficacy calibration
Figure S4. Neratinib does fractionation

REFERENCES

[1] S. Chakrabarti and F. Michor, "Pharmacokinetics and Drug Interactions Determine Optimum Combination Strategies in Computational Models of Cancer Evolution," *Cancer Res.*, vol. 77, no. 14, pp. 3908–3921, Jul. 2017, doi: 10.1158/0008-5472.CAN-16-2871.

[2] H. Weedon-Fekjær, B. H. Lindqvist, L. J. Vatten, O. O. Aalen, and S. Tretli, "Breast cancer tumor growth estimated through mammography screening data," *Breast Cancer Res.*, vol. 10, no. 3, p. R41, Jun. 2008, doi: 10.1186/bcr2092.

[3] J. Zhang, J. J. Cunningham, J. S. Brown, and R. A. Gatenby, "Integrating evolutionary dynamics into treatment of metastatic castrate-resistant prostate cancer," *Nat. Commun.*, vol. 8, no. 1, p. 1816, Nov. 2017, doi: 10.1038/s41467-017-01968-5.

[4] M. Hafner, M. Niepel, M. Chung, and P. K. Sorger, "Growth rate inhibition metrics correct for confounders in measuring sensitivity to cancer drugs," *Nat. Methods*, vol. 13, no. 6, pp. 521–527, Jun. 2016, doi: 10.1038/nmeth.3853.

[5] R. Diegmiller, L. Salphati, B. Alicke, T. R. Wilson, T. J. Stout, and M. Hafner, "Growth-rate model predicts in vivo tumor response from in vitro data," *CPT Pharmacomet. Syst. Pharmacol.*, p. psp4.12836, Jul. 2022, doi: 10.1002/psp4.12836.

[6] "Nerlynx (neratinib maleate) Tablets Drug Approval Package," US Food & Drug Administration Center for Drug Evaluation and Research, 208051, Jul. 2017. [Online]. Available: https://www.accessdata.fda.gov/drugsatfda_docs/nda/2017/208051Orig1s000TOC.cfm

[7] J. Zhang and K. Koch, "Population Pharmacokinetics of Lapatinib in Cancer Patients," presented at the Population Approach Group Europe, PAGE 20, 2011.

[8] S. G. Summerfield, J. W. T. Yates, and D. A. Fairman, "Free Drug Theory - No Longer Just a Hypothesis?," *Pharm. Res.*, vol. 39, no. 2, pp. 213–222, Feb. 2022, doi: 10.1007/s11095-022-03172-7.

[9] "Tykerb (Lapatinib) Tablets Drug Approval Package," US Food & Drug Administration Center for Drug Evaluation and Research, 022059, Mar. 2007. [Online]. Available: https://www.accessdata.fda.gov/drugsatfda_docs/nda/2007/022059s000_ClinPharmR.pdf

[10] V. Sopik and S. A. Narod, "The relationship between tumour size, nodal status and distant metastases: on the origins of breast cancer," *Breast Cancer Res. Treat.*, vol. 170, no. 3, pp. 647–656, Aug. 2018, doi: 10.1007/s10549-018-4796-9.

[11] Z. Varga, A. Noske, C. Ramach, B. Padberg, and H. Moch, "Assessment of HER2 status in breast cancer: overall positivity rate and accuracy by fluorescence in situ hybridization and immunohistochemistry in a single institution over 12 years: a quality control study," *BMC Cancer*, vol. 13, no. 1, p. 615, Dec. 2013, doi: 10.1186/1471-2407-13-615.

[12] C. Mills *et al.*, "Multiplexed and reproducible high content screening of live and fixed cells using the Dye Drop method," In Review, preprint, Jul. 2022. doi: 10.21203/rs.3.rs-1813095/v1.

[13] X. Dai, H. Cheng, Z. Bai, and J. Li, "Breast Cancer Cell Line Classification and Its Relevance with Breast Tumor Subtyping," *J. Cancer*, vol. 8, no. 16, pp. 3131–3141, 2017, doi: 10.7150/jca.18457.

[14] J. S. Spratt, J. S. Meyer, and J. A. Spratt, "Rates of growth of human neoplasms: Part II," *J. Surg. Oncol.*, vol. 61, no. 1, pp. 68–83, Jan. 1996, doi: 10.1002/1096-9098(199601)61:1<68::AID-JSO2930610102>3.0.CO;2-E.

[15] E. A. Eisenhauer *et al.*, "New response evaluation criteria in solid tumours: revised RECIST guideline (version 1.1)," *Eur. J. Cancer Oxf. Engl. 1990*, vol. 45, no. 2, pp. 228–247, Jan. 2009, doi: 10.1016/j.ejca.2008.10.026.

[16] M. Martin *et al.*, "A phase two randomised trial of neratinib monotherapy versus lapatinib plus capecitabine combination therapy in patients with HER2+ advanced breast cancer," *Eur. J. Cancer Oxf. Engl. 1990*, vol. 49, no. 18, pp. 3763–3772, Dec. 2013, doi: 10.1016/j.ejca.2013.07.142.

[17] K. Keyvanjah *et al.*, "Pharmacokinetics and safety of neratinib during co-administration with loperamide in healthy subjects," *Cancer Chemother. Pharmacol.*, vol. 84, no. 5, pp. 1125–1132, Nov. 2019, doi: 10.1007/s00280-019-03951-x.

[18] S. Litière, E. G. E. de Vries, L. Seymour, D. Sargent, L. Shankar, and J. Bogaerts, "The components of progression as explanatory variables for overall survival in the Response Evaluation Criteria in Solid Tumours 1.1 database," *Eur. J. Cancer*, vol. 50, no. 10, pp. 1847–1853, Jul. 2014, doi: 10.1016/j.ejca.2014.03.014.

[19] G. Bon *et al.*, "Loss of HER2 and decreased T-DM1 efficacy in HER2 positive advanced breast cancer treated with dual HER2 blockade: the SePHER Study," *J. Exp. Clin. Cancer Res. CR*, vol. 39, no. 1, p. 279, Dec. 2020, doi: 10.1186/s13046-020-01797-3.

[20] M. Toi *et al.*, "Lapatinib monotherapy in patients with relapsed, advanced, or metastatic breast cancer: efficacy, safety, and biomarker results from Japanese patients phase II studies," *Br. J. Cancer*, vol. 101, no. 10, pp. 1676–1682, Nov. 2009, doi: 10.1038/sj.bjc.6605343.

[21] H. J. Burstein *et al.*, "A phase II study of lapatinib monotherapy in chemotherapy-refractory HER2-positive and HER2-negative advanced or metastatic breast cancer," *Ann. Oncol.*, vol. 19, no. 6, pp. 1068–1074, Jun. 2008, doi: 10.1093/annonc/mdm601.

[22] K. M. Koch *et al.*, "Effects of Food on the Relative Bioavailability of Lapatinib in Cancer Patients," *J. Clin. Oncol.*, vol. 27, no. 8, pp. 1191–1196, Mar. 2009, doi: 10.1200/JCO.2008.18.3285.

[23] O. M. Filho *et al.*, "Impact of HER2 Heterogeneity on Treatment Response of Early-Stage HER2-Positive Breast Cancer: Phase II Neoadjuvant Clinical Trial of T-DM1 Combined with Pertuzumab," *Cancer Discov.*, vol. 11, no. 10, pp. 2474–2487, Oct. 2021, doi: 10.1158/2159-8290.CD-20-1557.

[24] M. Nishino *et al.*, "Tumor Growth Rate After Nadir Is Associated With Survival in Patients With EGFR-Mutant Non-Small-Cell Lung Cancer Treated With Epidermal Growth Factor Receptor Tyrosine Kinase Inhibitor," *JCO Precis. Oncol.*, vol. 5, pp. 1603–1610, Nov. 2021, doi: 10.1200/PO.21.00172.

[25] R. L. Yong *et al.*, "Residual tumor volume and patient survival following reoperation for recurrent glioblastoma," *J. Neurosurg.*, vol. 121, no. 4, pp. 802–809, Oct. 2014, doi: 10.3171/2014.6.JNS132038.

[26] S. M. Krishnan, S. S. Laarif, B. C. Bender, A. L. Quartino, and L. E. Friberg, "Tumor growth inhibition modeling of individual lesion dynamics and interorgan variability in HER2-negative breast cancer patients treated with docetaxel," *CPT Pharmacomet. Syst. Pharmacol.*, vol. 10, no. 5, pp. 511–521, May 2021, doi: 10.1002/psp4.12629.

[27] J. Zhou, Q. Li, and Y. Cao, “Spatiotemporal Heterogeneity across Metastases and Organ-Specific Response Informs Drug Efficacy and Patient Survival in Colorectal Cancer,” *Cancer Res.*, vol. 81, no. 9, pp. 2522–2533, May 2021, doi: 10.1158/0008-5472.CAN-20-3665.

[28] J. Zhou, Y. Liu, Y. Zhang, Q. Li, and Y. Cao, “Modeling Tumor Evolutionary Dynamics to Predict Clinical Outcomes for Patients with Metastatic Colorectal Cancer: A Retrospective Analysis,” *Cancer Res.*, vol. 80, no. 3, pp. 591–601, Feb. 2020, doi: 10.1158/0008-5472.CAN-19-1940.

[29] N. L. Spector *et al.*, “Lapatinib Plasma and Tumor Concentrations and Effects on HER Receptor Phosphorylation in Tumor,” *PloS One*, vol. 10, no. 11, p. e0142845, 2015, doi: 10.1371/journal.pone.0142845.

[30] D. K. Meijer and P. Van der Sluijs, “The influence of binding to albumin and alpha 1-acid glycoprotein on the clearance of drugs by the liver,” *Pharm. Weekbl. Sci.*, vol. 9, no. 2, pp. 65–74, Apr. 1987, doi: 10.1007/BF01960738.

[31] A. Sparreboom, K. Nooter, W. J. Loos, and J. Verweij, “The (ir)relevance of plasma protein binding of anticancer drugs,” *Neth. J. Med.*, vol. 59, no. 4, pp. 196–207, Oct. 2001, doi: 10.1016/s0300-2977(01)00157-7.

[32] T. Fujii *et al.*, “Implications of Low Serum Albumin as a Prognostic Factor of Long-term Outcomes in Patients With Breast Cancer,” *Vivo Athens Greece*, vol. 34, no. 4, pp. 2033–2036, Aug. 2020, doi: 10.21873/invivo.12003.

[33] J. W. Polli *et al.*, “The role of efflux and uptake transporters in [N-{3-chloro-4-[(3-fluorobenzyl)oxy]phenyl}-6-[5-({[2-(methylsulfonyl)ethyl]amino}methyl)-2-furyl]-4-quinazolinamine (GW572016, lapatinib) disposition and drug interactions,” *Drug Metab. Dispos. Biol. Fate Chem.*, vol. 36, no. 4, pp. 695–701, Apr. 2008, doi: 10.1124/dmd.107.018374.

[34] B. T. Li *et al.*, “HER2-Mediated Internalization of Cytotoxic Agents in ERBB2 Amplified or Mutant Lung Cancers,” *Cancer Discov.*, vol. 10, no. 5, pp. 674–687, May 2020, doi: 10.1158/2159-8290.CD-20-0215.

[35] D. Zhang *et al.*, “Drug Concentration Asymmetry in Tissues and Plasma for Small Molecule-Related Therapeutic Modalities,” *Drug Metab. Dispos. Biol. Fate Chem.*, vol. 47, no. 10, pp. 1122–1135, Oct. 2019, doi: 10.1124/dmd.119.086744.

[36] X. Liu, M. Wright, and C. E. C. A. Hop, “Rational Use of Plasma Protein and Tissue Binding Data in Drug Design: Miniperspective,” *J. Med. Chem.*, vol. 57, no. 20, pp. 8238–8248, Oct. 2014, doi: 10.1021/jm5007935.

[37] S. Stein, R. Zhao, H. Haeno, I. Vivanco, and F. Michor, “Mathematical modeling identifies optimum lapatinib dosing schedules for the treatment of glioblastoma patients,” *PLOS Comput. Biol.*, vol. 14, no. 1, p. e1005924, Jan. 2018, doi: 10.1371/journal.pcbi.1005924.

[38] X. Li *et al.*, “Comprehensive Analysis of EGFR-Mutant Abundance and Its Effect on Efficacy of EGFR TKIs in Advanced NSCLC with EGFR Mutations,” *J. Thorac. Oncol. Off. Publ. Int. Assoc. Study Lung Cancer*, vol. 12, no. 9, pp. 1388–1397, Sep. 2017, doi: 10.1016/j.jtho.2017.06.006.

[39] Y. Liu *et al.*, “EGFR mutation types and abundance were associated with the overall survival of advanced lung adenocarcinoma patients receiving first-line tyrosine kinase inhibitors,” *J. Thorac. Dis.*, vol. 14, no. 6, pp. 2254–2267, Jun. 2022, doi: 10.21037/jtd-22-755.

FIGURES

Figure 1. Virtual patients reflect real-world sources of variability

A. Variability in drug pharmacokinetics, target fraction, subpopulation growth rates, and drug-specific subpopulation sensitivity were considered during model development. Lapatinib and neratinib population PK models were adapted from publications by the original developers and FDA review documents. Target fraction (subpopulation proportions) was determined using HER2 IHC2/IHC3+ frequencies available in the literature [11]. Growth rates were derived from a published tumor growth model built on breast cancer screening data from 395,188 women [2]. Drug sensitivity for tumor subpopulations was obtained from GR metrics reported in the literature [4], [12].
B. Baseline tumor diameter at diagnosis (left) and the likelihood of metastatic disease at diagnosis based on baseline tumor diameter (center) used to calculate baseline tumor diameter at diagnosis of metastatic disease (right). Baseline tumor diameter frequencies below 20 mm were available in increments of 1 mm; above 20 mm were available in increments of 10 mm [10].
C. Simulated growth (red) of 15 mm diameter tumors as compared to [2] (black). Dashed lines indicate 5^{th}, 25^{th}, 75^{th}, and 95^{th} percentiles of 100 simulated tumors, while solid lines indicate medians.
D. Relative frequency of IHC3+ and FISH-amplified IHC2+ breast cancers at diagnosis reported in [11].

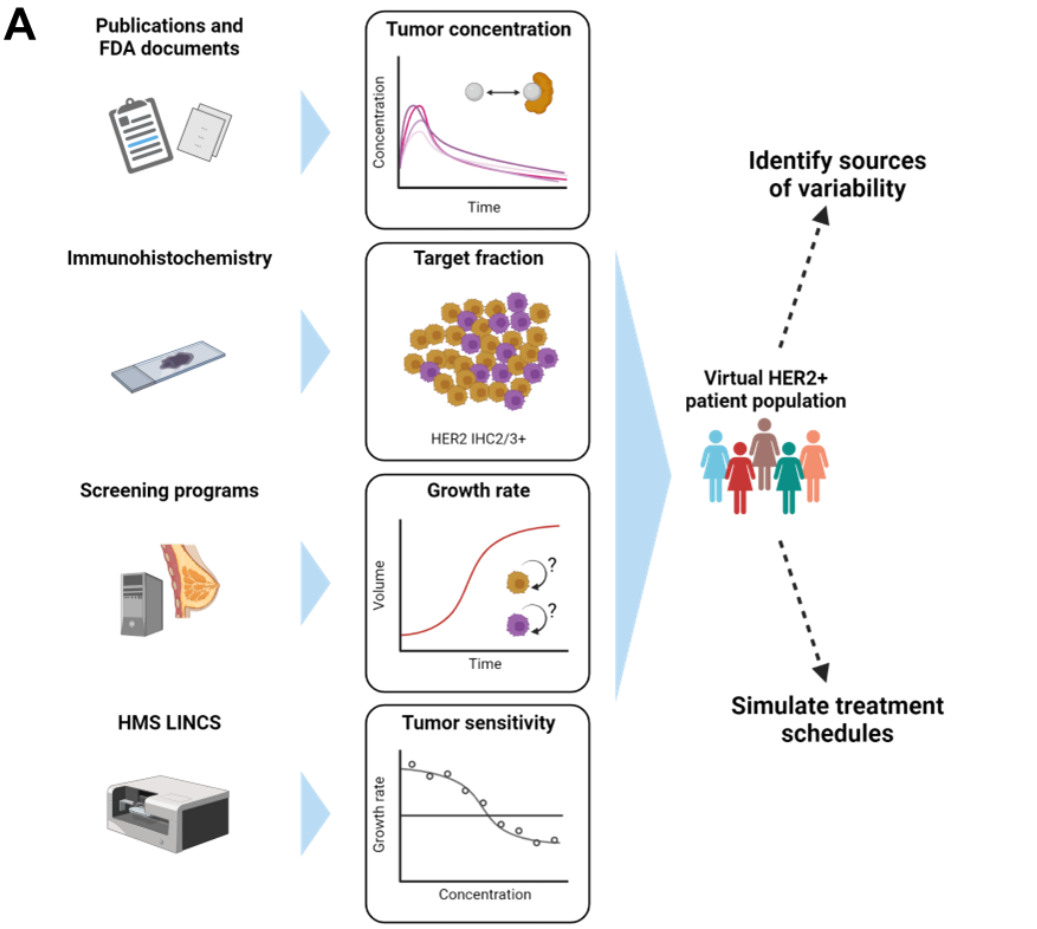
A
Publications and FDA documents
Tumor concentration
Concentration
Time
Immunohistochemistry
Target fraction
HER2 IHC2/3+
Screening programs
Growth rate
Volume
Time
HMS LINCS
Tumor sensitivity
Growth rate
Concentration
Identify sources of variability
Virtual HER2+ patient population
Simulate treatment schedules

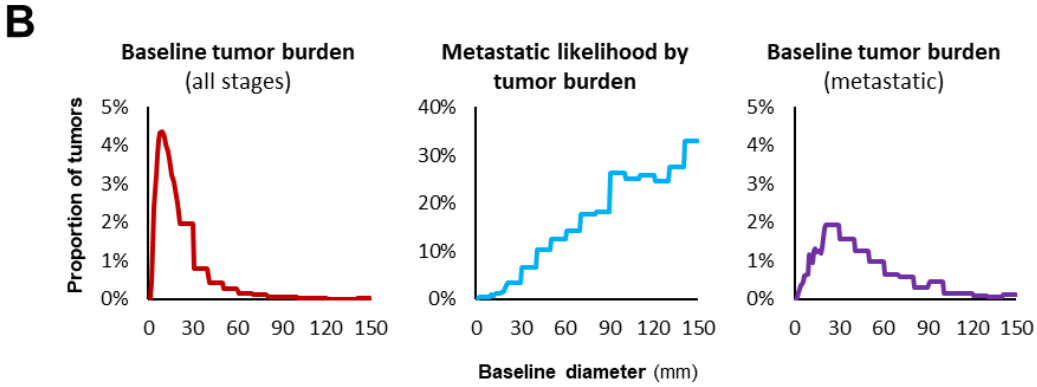
B
Baseline tumor burden (all stages)
Metastatic likelihood by tumor burden
Baseline tumor burden (metastatic)
Proportion of tumors
5%
4%
3%
2%
1%
0%
40%
30%
20%
10%
0
30
60
90
120
150
Baseline diameter (mm)

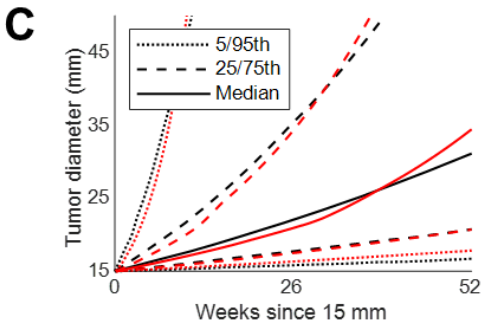
C
5/95th
25/75th
Median
Tumor diameter (mm)
45
35
25
15
0
26
52
Weeks since 15 mm

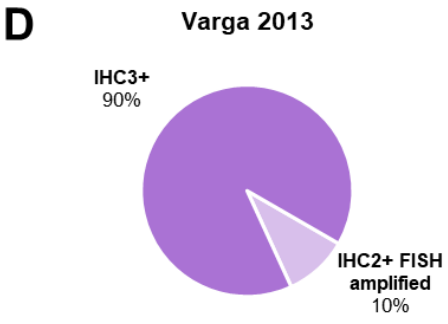
D
Varga 2013
IHC3+
90%
IHC2+ FISH amplified
10%

715

Figure 2. Tumor sensitivity and resistance to targeted therapies is heterogenous

A. Protein binding (PPB)-adjusted sensitivity (log_{10} nM) of breast cancer cell lines to six drugs approved for the treatment of metastatic breast cancer [4], [12]. Dashed lines indicate estimated average steady-state concentrations of free drug ($C_{ss,free}$). Inset percentages indicate the proportion of cell lines in the dataset with PPB-adjusted GEC_{50} below the drug's free $C_{ss,free}$. For visualization purposes, cell lines with no detected sensitivity to a particular drug at tested concentrations were assigned a nominal value of 1×10^9.

B. Neratinib GEC_{50} (left) and GR_{inf} (center) values for breast cancer cell lines reported in [12]. HER2 status was determined by [13]. Cell lines with conflicting HER2 status in the literature were excluded. $GR_{expected}$ (right) values reflect the predicted GR of each cell line at the estimated $C_{ss,avg}$ of neratinib.

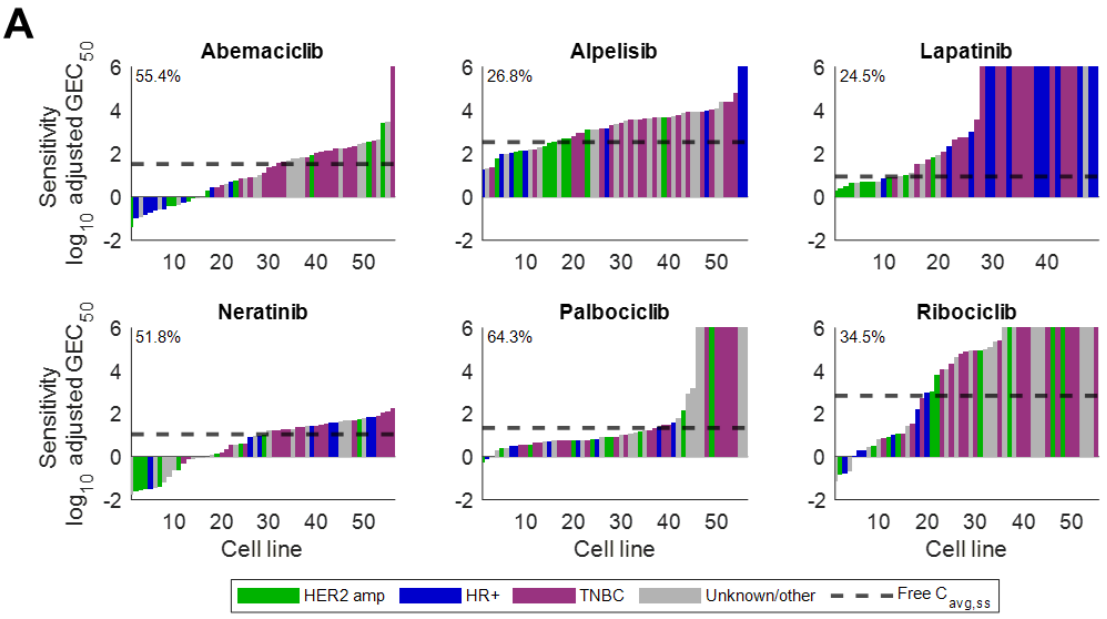
A
Abemaciclib
Alpelisib
Lapatinib
Neratinib
Palbociclib
Ribociclib
55.4%
26.8%
24.5%
51.8%
64.3%
34.5%
Sensitivity
log10 adjusted GEC50
Cell line
HER2 amp
HR+
TNBC
Unknown/other
Free Cavg,ss

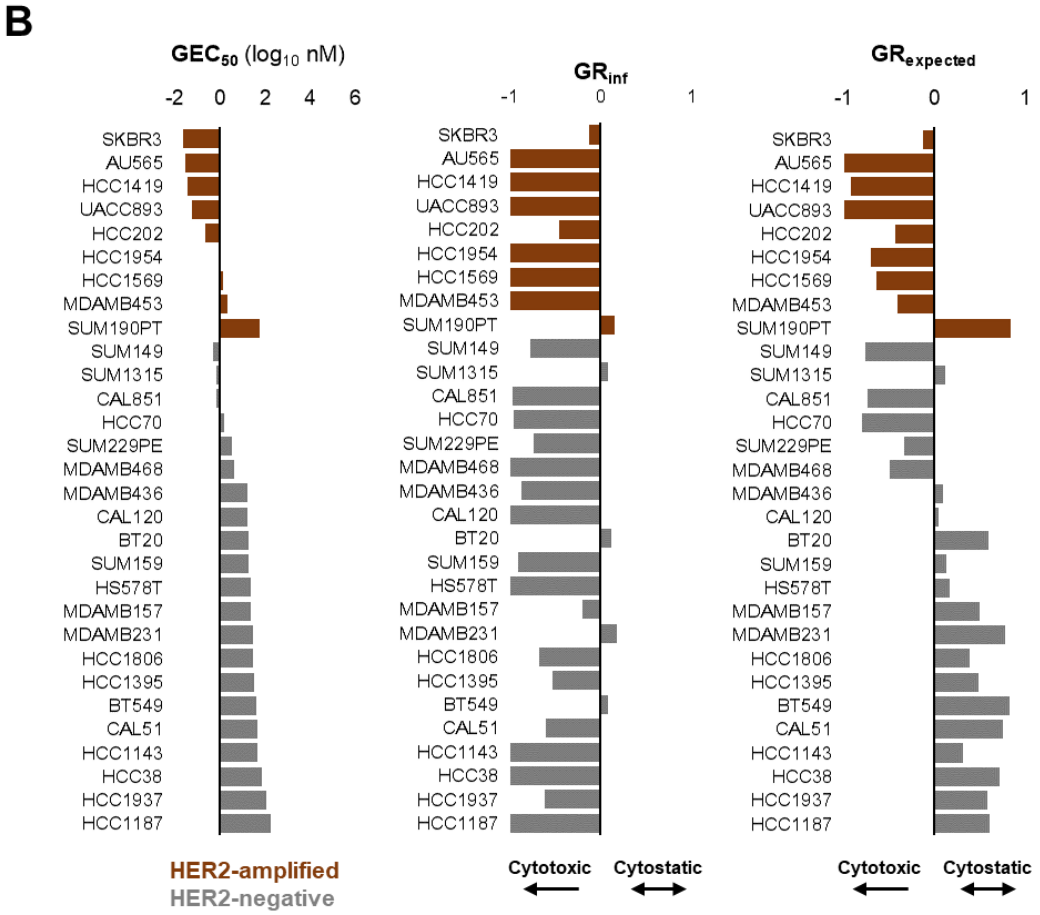
B
GEC50 (log10 nM)
GRinf
GRexpected
SKBR3
AU565
HCC1419
UACC893
HCC202
HCC1954
HCC1569
MDAMB453
SUM190PT
SUM149
SUM1315
CAL851
HCC70
SUM229PE
MDAMB468
MDAMB436
CAL120
BT20
SUM159
HS578T
MDAMB157
MDAMB231
HCC1806
HCC1395
BT549
CAL51
HCC1143
HCC38
HCC1937
HCC1187
HER2-amplified
HER2-negative
Cytotoxic
Cytostatic

Figure 3. PK/PD/TG model recapitulates the clinical efficacy of neratinib

A. Population pharmacokinetic model structure for neratinib reported in [6]. Drug absorption occurs through a first-order (K_a) process with delay (T_{lag}). Drug subsequently distributes (Q) between central/plasma (V_c) and peripheral (V_p) compartments and clears from the central compartment by first-order elimination (CL).
B. Simulated pharmacokinetic profiles during the first week of once-daily treatment with 240 mg neratinib. Lines represent medians, whereas shaded regions represent 5th and 95th percentiles. Black circles represent observations from [17].
C. Pharmacodynamic model of tumor growth comprising two competing cell populations with differential sensitivity to a cytostatic drug.
D. Growth dynamics of HER2-amplified ("sensitive") and HER2-negative ("resistant") subpopulations within an illustrative IHC2+ tumor. Values for either subpopulation are normalized to their abundance at treatment initiation.
E. Predicted PFS during 52 weeks of treatment with 240 mg QD neratinib using free drug-driven pharmacodynamics, compared to [16]. Only progression from target lesions is included.
F. Predicted ORR during 5 weeks of treatment with 240 mg QD neratinib using free drug-driven pharmacodynamics, compared to [16].
G. (E) with an additional daily chance of Death or Non-target Progression (DNTP) estimated as 1.5 x 10^{-4} events/mm of tumor diameter/day.
H. Risk of progression by source during each 6-week scan interval during 52 weeks of treatment with 240 mg QD neratinib. NAR, number at risk during the scan interval.

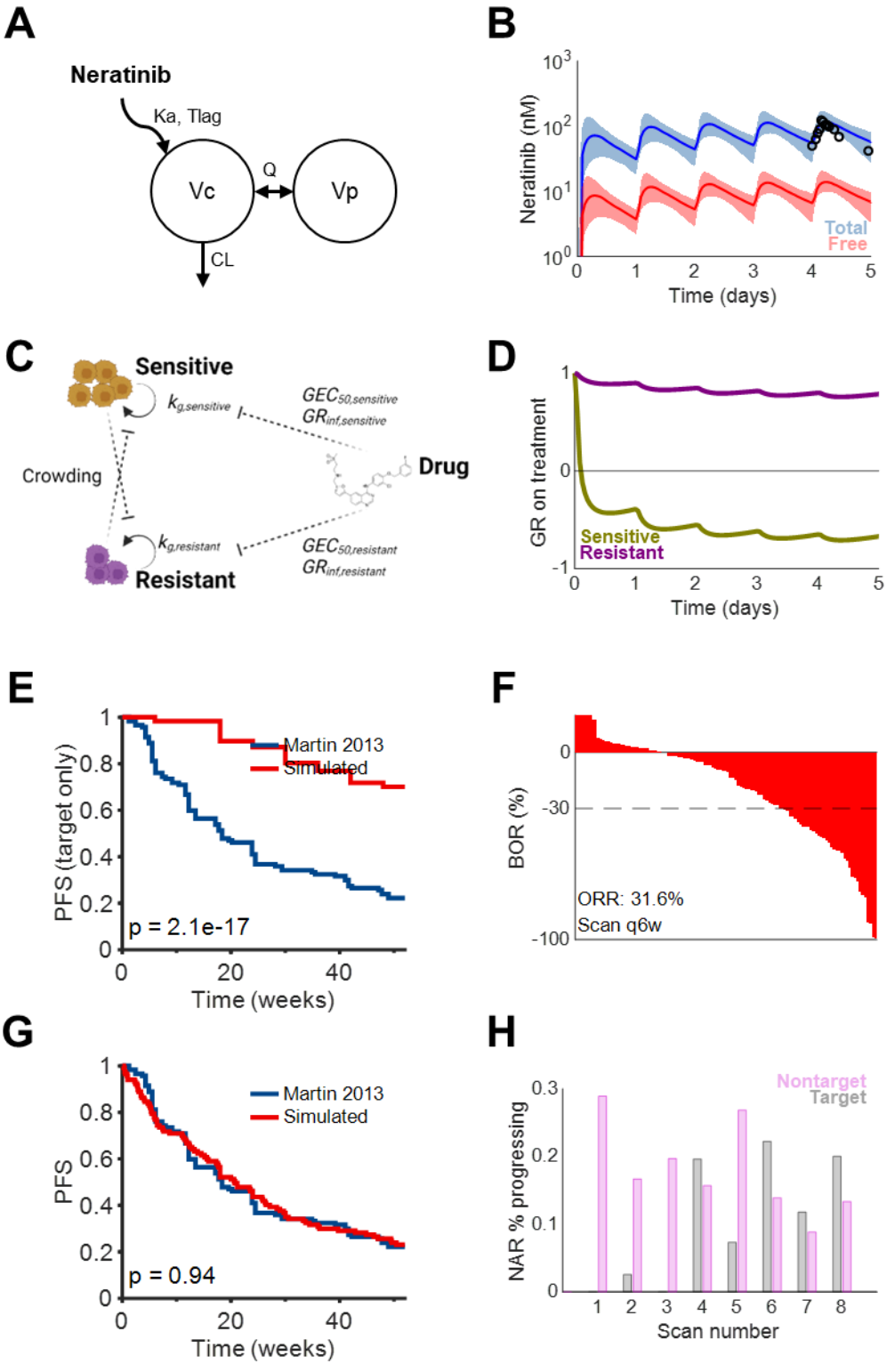
A
Neratinib
Ka, Tlag
Vc
Q
Vp
CL
B
Neratinib (nM)
Total
Free
Time (days)
C
Sensitive
Crowding
Drug
Resistant
D
GR on treatment
Sensitive
Resistant
Time (days)
E
PFS (target only)
Martin 2013
Simulated
p = 2.1e-17
Time (weeks)
F
BOR (%)
ORR: 31.6%
Scan q6w
G
PFS
Martin 2013
Simulated
p = 0.94
Time (weeks)
H
NAR % progressing
Nontarget
Target
Scan number

Figure 4. Tumor-intrinsic characteristics influence neratinib efficacy

A. Simulated PFS of 1000 patients with and without 52 weeks of treatment with 240 mg QD neratinib.
B. DNTP-free survival for each patient in untreated (blue) and treated (orange) states. DNTP-free survival is the time on study without a DNTP event.
C. Multiplicity-corrected significance of differences in PFS between patients with parameter values above or below the population median (bars). The dashed line represents the Benjamin-Hochberg significance threshold for one-way ANOVA. For visualization purposes, the y axis is truncated at 2.5.
D. Significant differences in PFS stratified by tumor burden (left), resistant cell growth rate (middle), sensitive cell GEC_{50} (right) quartiles.
E. Normalized tumor diameters (left), sensitive cell volume (middle), and resistant cell volume (right) stratified length of PFS relative to median PFS (mPFS). All y axes are on a log scale. Shaded regions represent interquartile ranges.
F. Representative profiles of baseline-normalized sensitive and resistant cell abundance from three virtual patients treated with 52 weeks of 240 mg QD neratinib.

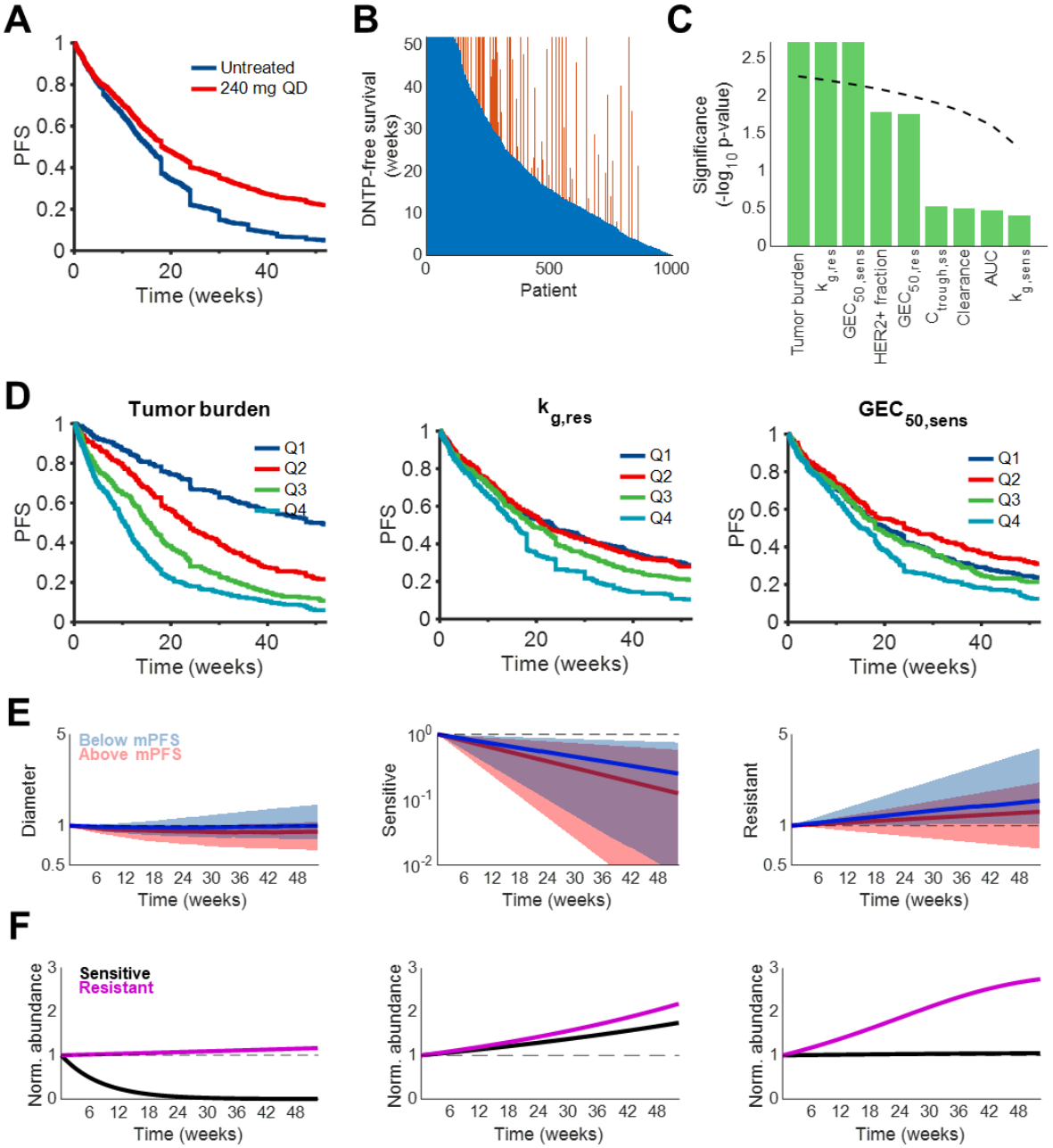
A
Untreated
240 mg QD
PFS
Time (weeks)
B
DNTP-free survival (weeks)
Patient
C
Significance (-log10 p-value)
Tumor burden
kg,res
GEC50,sens
HER2+ fraction
GEC50,res
Ctrough,ss
Clearance
AUC
kg,sens
D
Tumor burden
kg,res
GEC50,sens
Q1
Q2
Q3
Q4
PFS
Time (weeks)
E
Below mPFS
Above mPFS
Diameter
Sensitive
Resistant
Time (weeks)
F
Sensitive
Resistant
Norm. abundance
Time (weeks)

Figure 5. Different tumor-intrinsic characteristics influence lapatinib efficacy

A. Population pharmacokinetic model structure for lapatinib reported in [7]. Drug absorption occurs through a sequential zero-order (Dur) and first-order (K_a) process with delay (T_{lag}). Drug subsequently distributes (Q) between central/plasma (V_c) and peripheral (V_p) compartments and clears from the central compartment by first-order elimination (CL).
B. Simulated pharmacokinetic profiles during the first week of once-daily treatment with 1500 mg lapatinib. Lines represent medians, whereas shaded regions represent 5^{th} and 95^{th} percentiles. Black circles represent observations from [22].
C. Simulated PFS of 1000 patients with and without treatment of 1500 mg daily lapatinib.
D. DNTP-free survival for each patient in untreated (blue) and treated (orange) states. DNTP-free survival is the time on study without a DNTP event.
E. Multiplicity-corrected significance of differences in PFS between patients with parameter values above or below the population median (bars). The dashed line represents the Benjamin-Hochberg significance threshold for one-way ANOVA. For visualization purposes, the y axis is truncated at 2.5.
F. Significant differences in PFS stratified by tumor burden (left), resistant cell growth rate (middle), sensitive cell HER2+ fraction (right) quartiles.
G. Normalized tumor diameters (left), sensitive cell volume (middle), and resistant cell volume (right) stratified length of PFS relative to median PFS (mPFS). All y axes are on a log scale. Shaded regions represent interquartile ranges.

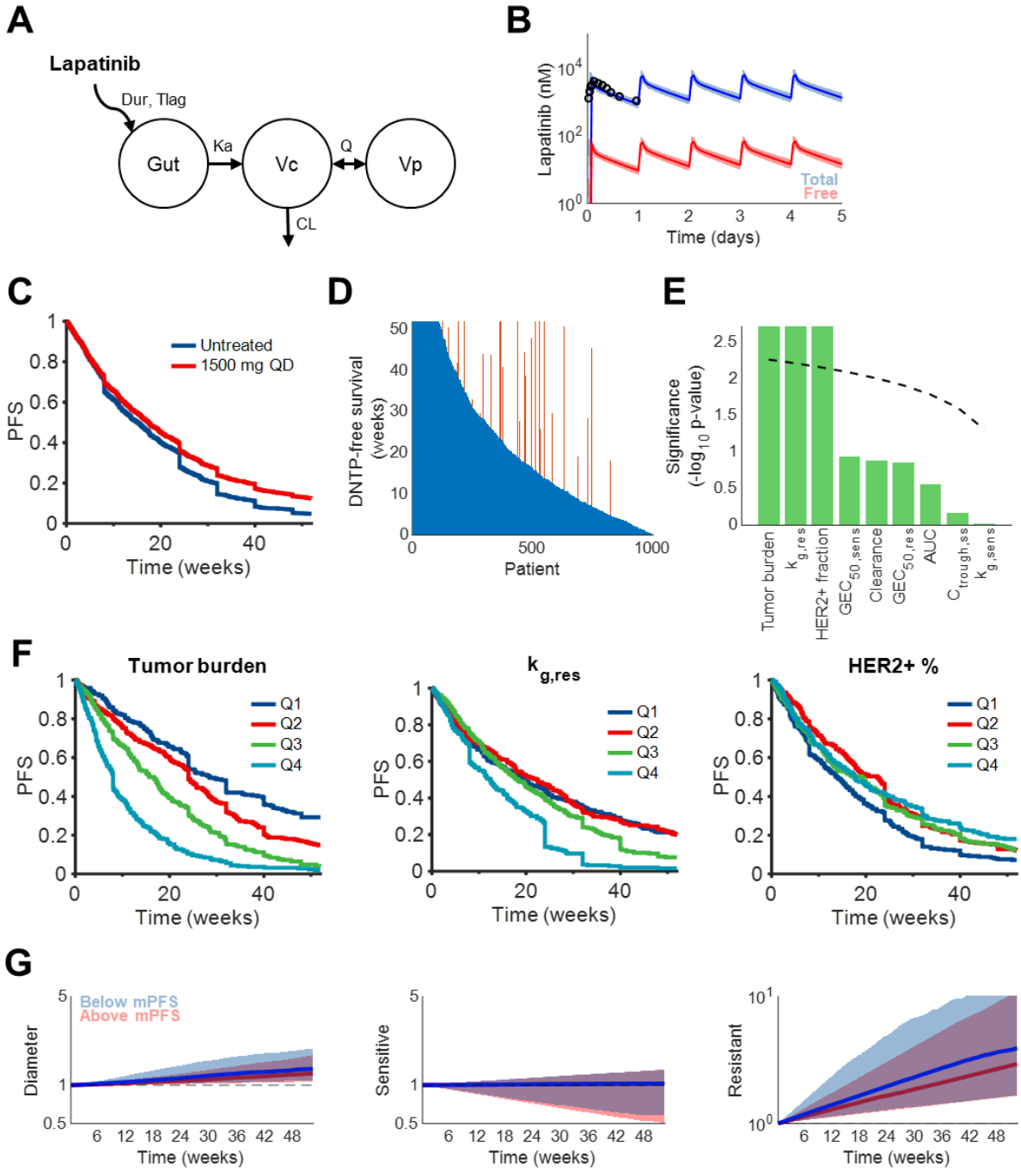
A
Lapatinib
Dur, Tlag
Gut
Ka
Vc
Q
Vp
CL
B
Lapatinib (nM)
Total
Free
Time (days)
C
Untreated
1500 mg QD
PFS
Time (weeks)
D
DNTP-free survival (weeks)
Patient
E
Significance (-log10 p-value)
Tumor burden
kg,res
HER2+ fraction
GEC50,sens
Clearance
GEC50,res
AUC
Ctrough,ss
kg,sens
F
Tumor burden
kg,res
HER2+ %
Q1
Q2
Q3
Q4
PFS
Time (weeks)
G
Below mPFS
Above mPFS
Diameter
Sensitive
Resistant
Time (weeks)

Figure 6. Dose intensification benefits neratinib more than lapatinib

A. PFS benefit from treatment with 240 mg QD or BID neratinib versus no treatment. PFS benefit is the positive difference in predicted PFS between two treatment schedules.

B. (A) for 1500 mg QD or BID lapatinib.

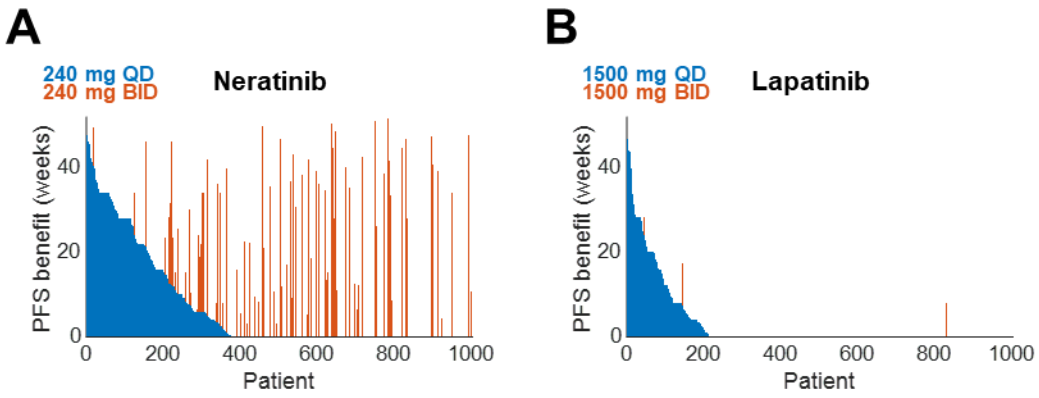

Figure S1. Lapatinib drug sensitivity

A. Lapatinib GEC_{50} (left) and GR_{inf} (center) values for breast cancer cell lines reported in [4]. HER2 status was determined by [13]. Cell lines with conflicting HER2 status in the literature were excluded. $GR_{expected}$ (right) values reflect the predicted GR of each cell line at the estimated $C_{ss,avg}$ of lapatinib.

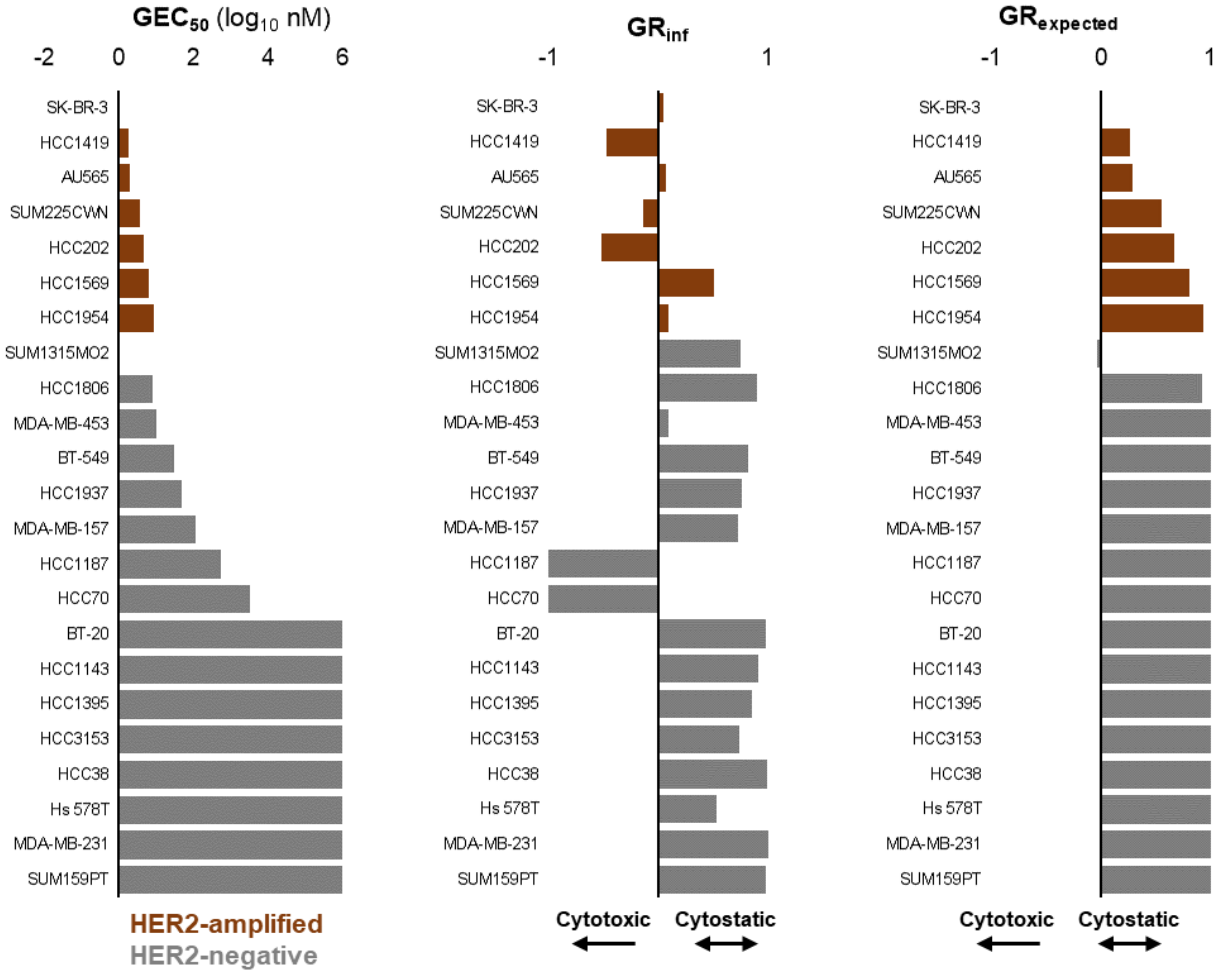

Figure S2. Neratinib pharmacodynamics using total or free drug

A. Predicted PFS (top) and ORR (bottom) during treatment with 240 mg daily neratinib using total drug-driven pharmacodynamics, compared to [16]. Only progression from target lesions is included.

B. (A) using free drug-driven pharmacodynamics.

C. (B) with an additional daily chance of Death or Non-target Progression (DNTP) estimated as 1.5 x 10^{-4} events/mm of tumor diameter/day.

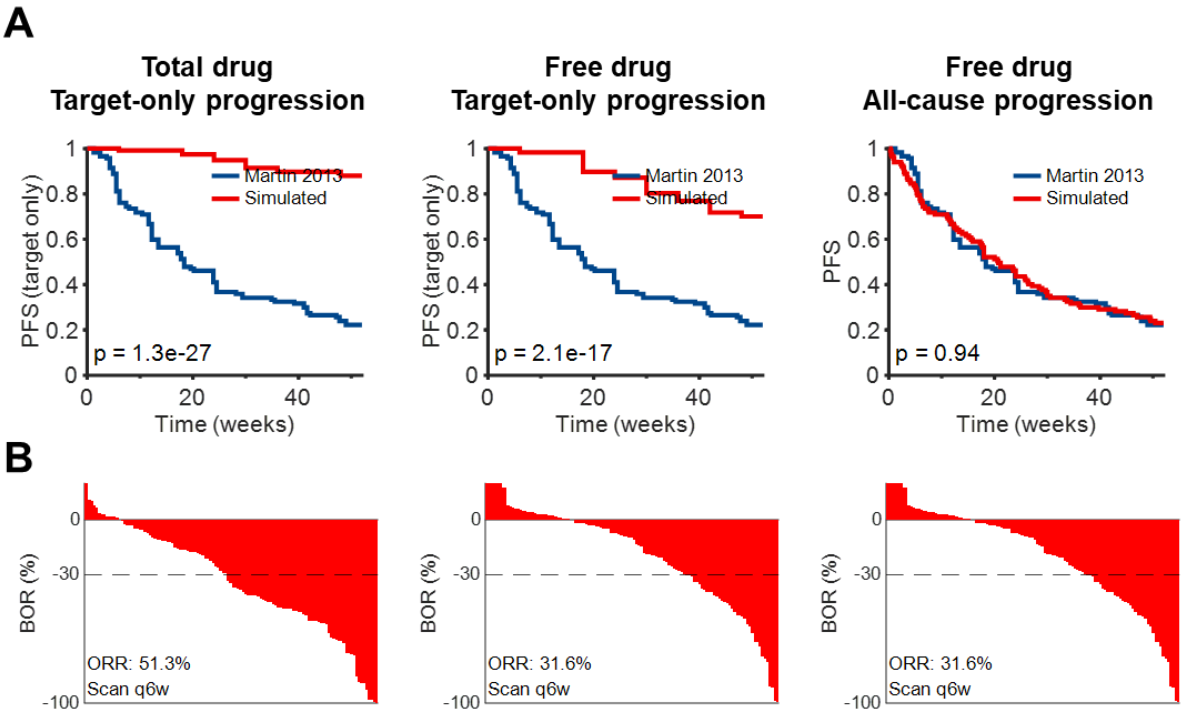

Figure S3. Lapatinib efficacy calibration

A. Predicted PFS (left) and ORR (right) of 1500 mg QD lapatinib using free-driven pharmacodynamics and an additional daily chance of Death or Non-target Progression (DNTP) estimated as 1.5×10^{-4} * tumor diameter in mm, compared to [20], [21].

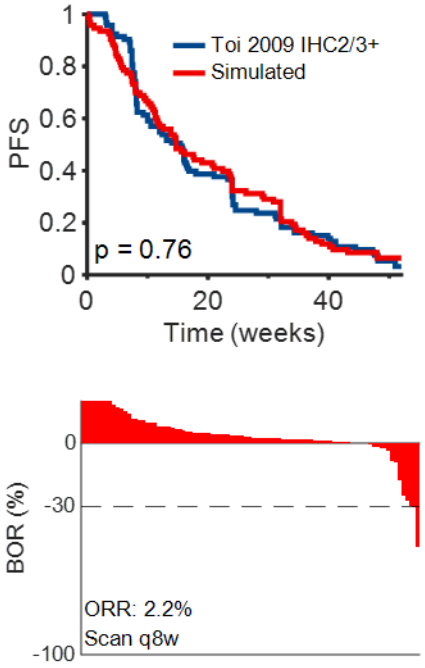

Figure S4. Neratinib dose fractionation

A. PFS benefit from treatment with 240 mg QD or 120 mg BID neratinib versus no treatment. PFS benefit is the positive difference in predicted PFS between two treatment schedules. Lack of orange bars indicates PFS equivalence between 240 mg QD and 120 mg BID.